General Disclaimer

One or more of the Following Statements may affect this Document

- This document has been reproduced from the best copy furnished by the organizational source. It is being released in the interest of making available as much information as possible.

- This document may contain data, which exceeds the sheet parameters. It was furnished in this condition by the organizational source and is the best copy available.

- This document may contain tone-on-tone or color graphs, charts and/or pictures, which have been reproduced in black and white.

- This document is paginated as submitted by the original source.

- Portions of this document are not fully legible due to the historical nature of some of the material. However, it is the best reproduction available from the original submission.

A HIGH RESOLUTION SOLAR ATLAS FOR FLUORESCENCE CALCULATIONS

Michael F. A'Hearn

John T. Ohlmacher

and

David G. Schleicher

Technical Report: TR AP83-044

29 July 1983

Astronomy Program

University of Maryland

College Park, MD   20942

USA

ERRATUM

A HIGH RESOLUTION SOLAR ATLAS FOR FLUORESCENCE CALCULATIONS

by A'Hearn, Ohlmacher and Schleicher

The Kitt Peak spectrum referred to in this report was not actually obtained by R. West as stated on page 12 and in the acknowledgements although he did bring the spectrum to our attention. The spectrum was obtained by J. Brault and L. Testerman of Kitt Peak as part of a more extensive study of the solar spectrum. The various data from their program are being synthesized into a more complete solar spectrum by R. L. Kurucz of Harvard. That work will include a more careful study of the absolute wavelengths as well as a wider spectral range and other considerations.

14 October 1983

I. INTRODUCTION

In the course of our program to study the fluorescence process in comets, we frequently require the solar spectrum at high spectral resolution in absolute units. For some programs, such as fluorescence of hydrogen in the Lyman-α line, only a small portion of the solar spectrum is needed, e.g., the few Angstroms including the Lyman-α line. At the other extreme, however, are molecules like C_2 and CO^+. These species have emission bands which extend from the ultraviolet to the red (CO^+) or even to the infrared (C_2). A proper calculation of the fluorescence by these molecules thus requires a homogeneous solar spectrum over this entire spectral range. In order to meet this need we have synthesized a solar spectrum from various sources.

There are a number of characteristics required in a solar atlas to be used for fluorescence calculations. In the first place, the spectrum must refer to the whole disc of the sun (i.e., the solar irradiance), not just the center of the sun. Secondly it must have a reasonably good calibration in absolute flux units. Thirdly, it must have a spectral resolution comparable to or better than the thermal widths expected for cometary specral lines and, in order to study the Greenstein effect in comets, the spectral resolution of the atlas must be better than the expected Doppler widths due to mass motions within the comet. The overall expansion of cometary material is expected to take place at velocities of order 1 km/sec while the expected sublimation temperatures, 150 to 200 K, imply thermal velocities of several tenths of a km/sec. Therefore, a spectral resolution of several tenths of a km/sec is appropriate for our purposes. This turns out to require unavailable data. Fortunately for us, the solar rotation (2 km/sec near the equator) smooths out all features finer than this. We can therefore accept a somewhat lower resolution, of order 1 km/sec, provided it is interpolated to better than 1 km/sec.

Our general approach has been to provide an absolute intensity calibration which is completely independent of the high resolution data which form the basis for our final spectrum. Several sources of low resolution data have been combined to provide an absolutely calibrated spectrum from 2250 Å to 7000 Å. Similarly three different sources of high resolution data are used to cover this same spectral range. We have used the low resolution data to put each high resolution spectrum on an absolute scale. We have then combined the three high resolution spectra in their overlap regions to produce a single, absolutely calibrated high resolution spectrum over the entire spectral range.

Although this atlas was assembled for our own purposes of calculating the fluorescence spectrum in comets, it does have other applications. Nicolet (1981), for example, has recently discussed the same problem from the viewpoint of photochemical rates relevant to aeronomy although he did not require spectral resolution nearly as high as ours. Similarly, these results are needed for fluorescence calculations relevant to planetary atmospheres and exospheres.

II. SOLAR VARIABILIY

An important question is whether or not the solar spectrum shows any variability that would matter for our purposes.

The only fluctuations which matter for our purposes are those which exceed a few percent on time scales from hours (the time required to establish fluorescent equilibrium for cometary species) to several decades (the time span of quantitative data on comets). Two recent conferences on solar variability* have considered many different types of variation. Examination of the proceedings leads one to conclude that, at least in the optical region, there are no changes in the solar spectrum relevant to our interests with the exception of changes in a few discrete absorption lines. For example, the intensity at the core of the Ca II K line does vary significantly with the solar cycle (Livingston, et al. 1981). Since this will matter only for transitions pumped at that frequency, none of which are of interest to us, we have ignored this effect. Fluctuations associated with the five minute oscillations (e.g., Fröhlich, 1981) are too rapid to be of interest to us.

In the ultraviolet, there are large (>30%) discrepancies among different observers. Simon (1981) has reviewed the various determinations, looking specifically for real variations. The best results should come from repeated measurements with the same instrument, such as those of Simon himself. He concludes that the variations with solar rotation (27-day period) are 1-2% for $\lambda 2400 - 3300$ Å (mainly at the discrete Fraunhofer lines of Mg II near 2800 Å) and 2-4% for $\lambda 2000 - 2400$ Å (mainly shortward of $\lambda 2100$ Å). These fluctuations are only of marginal significance for our purposes and the largest ones are

---

*XIVth ESLAB Symposium on "Physics of Solar Variations" Sept. 1980; Papers published as vol. 74 of Solar Physics. Workshop held at Goddard Space Flight Center Nov. 1980; Proceedings published as "Variations of the Solar Constant" ed. S. Sofia NASA Conf. Publ. 2191.

outside the spectral range under consideration (i.e., $\lambda < 2250$ Å). We will therefore neglect these changes. The longer term variability, specifically that with the 11-year solar cycle, is less well determined. Simon therefore gives only upper limits of 2% for the region $\lambda 2400 - 3300$ Å and 10% for the region $\lambda 2000 - 2400$ Å. Again the variation longward of $\lambda 2400$ is of only marginal significance and we neglect it. The upper limit for variations in the range $\lambda 2000 - 2400$ Å might be important for our purposes, but it is clear that with current data we cannot take these variations into account since they are not adequately determined.

In summary, the present atlas will make no attempt to take into account any variations with time. Such variations may be significant, however, at the core of certain lines such as the K-line and at wavelengths < 2400 Å. These limitations must be kept in mind when using the atlas.

III. ABSOLUTE FLUX CALIBRATIONS

The absolute calibration of the solar irradiance in the optical region
has been taken from the work of Neckel and Labs (1981). They have provided
the total irradiance at 1 AU integrated over 20 Å-wide bandpasses (20.5 Å-wide
for $\lambda < 4010$ Å). They have estimated the accuracy of their results as better
than 1% at most wavelengths and better than 2% in the near ultraviolet. Other
absolute spectra of the sun, however, differ from these results by much more
than 2%. The choice of the data from Neckel and Labs is strongly supported by
the work of Hardorp (1980). He has discussed in some detail the comparison
between the sun and other stars which resemble the sun, both in respect to the
overall flux distribution and also in the strength of two discrete absorption
features in the near ultraviolet region of the spectrum. The earlier calibra-
tion by Labs and Neckel (1968) was the only solar spectrum which could match
the overall flux distribution of any stars which had the solar strength for
the discrete features. In the course of that investigation, Hardorp uncovered
the small errors in their flux distribution which have been corrected in the
more recent work by Neckel and Labs. Although there may be uncertainties
larger than those cited by Neckel and Labs, it seems clear to us that these
data are by far the best available and that consequently there is no point in
averaging them with any other data.

In the ultraviolet, the situation is more ambiguous. The discrepancies
among different observers are larger and there is less basis for choosing one
over another. In their review of this quesion some years ago, Smith and
Gottlieb (1974) chose the work of Broadfoot (1972) as the best, but many more
recent sources of data are now available.

Since the discrepancies among different observers of the ultraviolet flux
distribution of the sun are much larger than the real variations, we must

select among the observers. In the spectral region λ2500 – 3000 Å, the data
of Broadfoot (1972) are in reasonably good agreement (10% or better) with a
variety of more recent data, particulary those of the groups headed by Simon
and by Heath (c.f. Nicolet, 1981; Simon, 1981) and from 2550 to 2900 Å they
are in good agreement with the results of Mount and Rottman (1981). In this
region, the results of Broadfoot are the highest of the various sets of data
but still in adequate agreement. The choice between these sources seems
arbitrary in this spectral range and we have adopted the results of
Broadfoot. We use only Broadfoot's Table 2, which contains averages over 10 Å
intervals, because his instrumental resolution was approximately 3 Å and his
wavelength scale also has uncertainties of 1 Å or more. Use of his Table 1
with data at 1 Å intervals would therefore require detailed knowledge of his
instrumental line shape whereas the 10 Å data can be considered (with 1%
accuracy) to have a rectangular line shape. Since the data of Broadfoot were
taken near aphelion, they should be increased by 3% to reduce them to 1 AU,
but we have omitted this correction on the grounds that Broadfoot's data are
systematically the highest of these sources by a comparable percentage.

Shortward of 2500 Å, there are serious discrepancies between the data of
Broadfoot, whose data are systematically highest, and a variety of other
sources. The data of Mount et al. (1980) are the lowest of the several
investigators and their values are roughly 2/3 of those of Broadfoot. Mount
et al. suggest that the discrepancy is due to scattered light in Broadfoot's
instrument, but if this were the case one might expect the size of the
discrepancy to be anticorrellated with the brightness and this is not the
case. The data from Heath and from Simon lie between those of Broadfoot and
those of Mount et al. (c.f. Nicolet, 1981, figs. 10a, 10b; Simon 1981, fig. 9)
but significantly closer to those of Broadfoot. We therefore ignore the

results of Mount et al. The selection among the other three is more
difficult. The results of Simon et al. (1982) might be questioned because
they were made at relatively low altitude (41 km) and therefore required
significant corrections for residual atmospheric absorption. They agree well,
however, with Heath's data taken from the Nimbus satellite (c.f., Simon
et al., fig. 2) indicating that these atmospheric c rrections were properly
applied. We conclude that in this spectral range, the data of Simon et al.
(1982) are as good as any and we use their average of the two most recent
measurements (their Table 2b).

We have now selected three sources of data for the absolute
calibration: Simon et al. (1982; Table 2b) for $\lambda < 2410$ Å; Broadfoot (1972;
Table 2) for the range $\lambda 2400 - 3200$ Å; Neckel and Labs (1981; Tables 2 and 3)
for the range $\lambda 3300 - 7000$ Å. It is still necessary to combine these data in
such a way as to eliminate a discontinuity at 2410 Å and to interpolate
between 3200 and 3300 Å. For the bandpass $\lambda 2353 - 2381$ Å, the value of Simon
et al. is .83 that of Broadfoot with no obvious trends in the ratio at shorter
wavelengths. To smoothly join with Broadfoot's data, we use Broadfoot's data
for the bands centered at 2390 through 2500 Å and multiply each by a value
which increases linearly from .83 at 2376 Å to 1.00 at 2500 Å. Above that
point, we take the values of Broadfoot and below $\lambda 2390$ we take the values of
Simon et al. The results of this splicing are given in Table 1 where we give
both the method of combining the sources and the actual values of the
result.

For the interpolation between Broadfoot's results shortward of 3200 Å and
those of Neckel and Labs longward of 3300 Å, we use the results of Simon
(1975, Table 1). These results are almost equal to those of Broadfoot short-
ward of 3000 Å and about 10% higher than those of Neckel and Labs at 3300 Å.

Since the data of Broadfoot seem to show a systematic drop from 3000 Å to
3200 Å but have much higher spectral resolution than those of Simon, we have
adopted a weighted average, as for the splicing at shorter wavelengths, with
the weights varying linearly from 100% Broadfoot/0% Simon at 3000 Å to 0%
Broadfoot/100% Simon at 3200 Å. We have then expressed this as a fraction of
Broadfoot's data which can then be interpolated with the results given in
Table 1. Similarly, we have used a weighting of 100% Simon/0% Neckel-Labs at
3250 Å linearly varying to 0% Simon/100% Neckel-Labs at 3400 Å.

The complete solar spectrum used for the calibration is given in
Table 1. Although some of the calibration was done in units of energy per
time per wavelength, the ultimate atlas (for our own convenience) has been
converted to radiation densities at 1 AU. These are the data given in
Table 1 in units of 10^{-24} erg cm^{-3} Hz^{-1} where the conversion of units was
done using λ at the center of the bandpass. The two wavelengths indicate
the range over which the original flux was integrated or averaged as
determined from the original reference. For all radiation densities greater
than 4000 x 10^{-24} ergs cm^{-3} Hz^{-1}, the numbers have been rounded to end in 0.
The results are also summarized graphically in Figure 1a where we have shown
the complete adopted calibration. Figure 1b shows, at expanded scales, the
short-wavelength portion of the calibration which includes all overlap
regions. In overlap regions, both original sources are shown as well as the
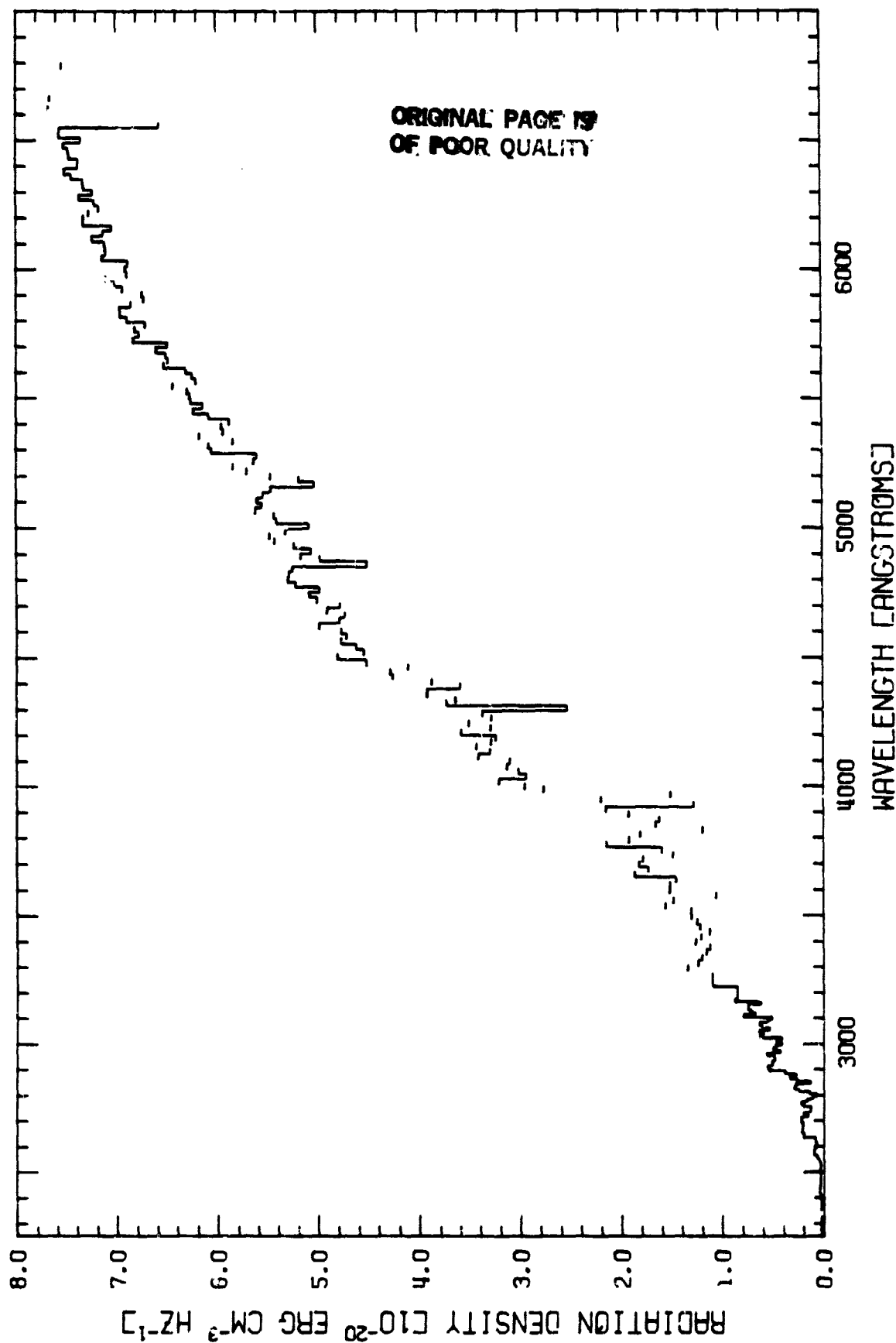adopted calibration.

Figure 1A: The adopted, absolute calibration of the solar spectrum, also listed in Table 1. Horizontal lines indicate widths of bandpasses. Vertical lines are absent if there is either a gap or an overlap between the adjacent band passes.

ABSOLUTE CALIBRATION OF THE SUN

×10

RADIATION DENSITY [10⁻²¹ ERG CM⁻³ HZ⁻¹]

$$\text{RADIATION DENSITY } [10^{-21} \text{ ERG CM}^{-3} \text{ HZ}^{-1}]$$
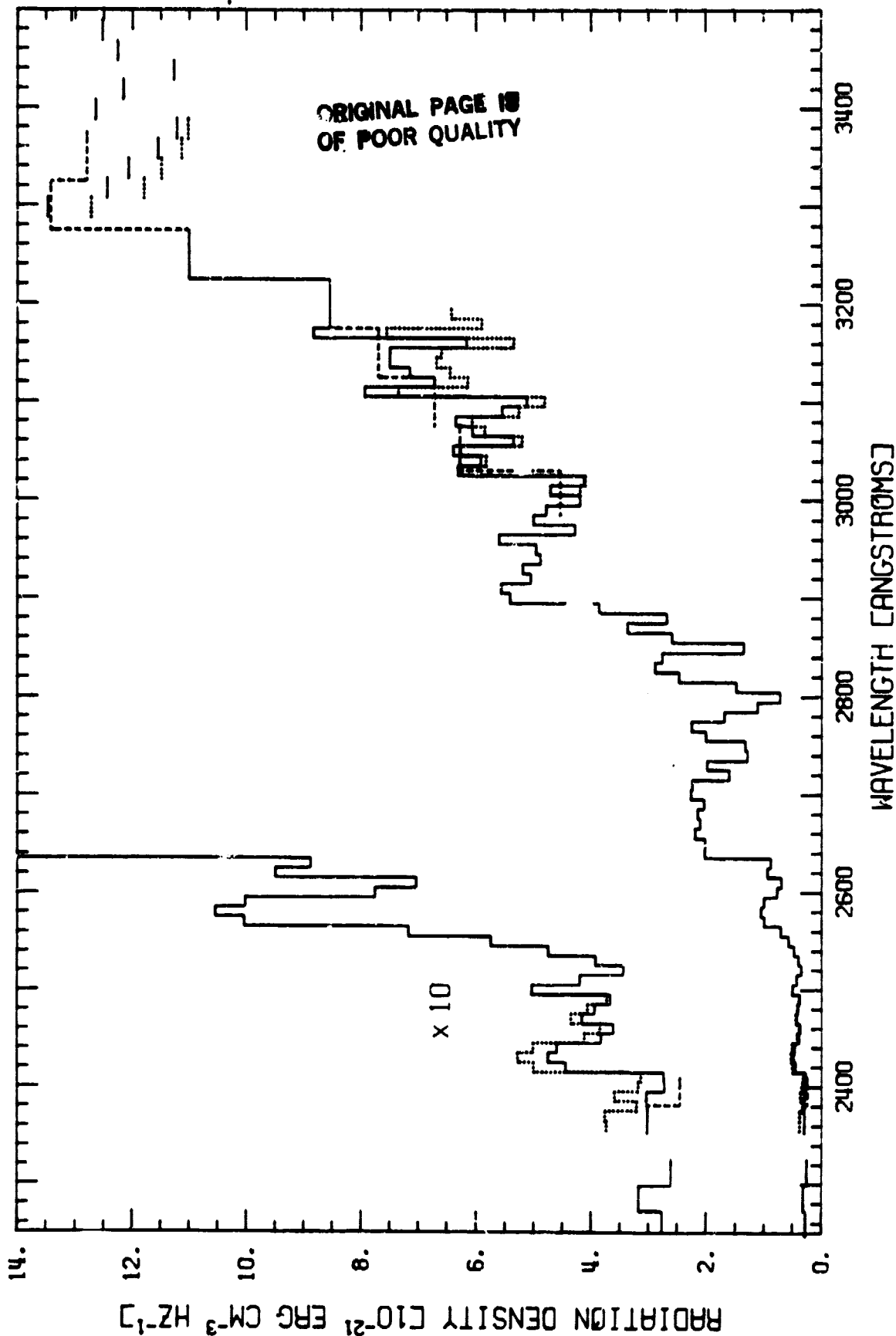
WAVELENGTH [ANGSTROMS]

Figure 13. The solid lines again indicate the adopted calibration. Both original sources are also shown in overlap regions, using broken lines for Simon, Pastiels, and Nevejans (1982) and for Simon (1975), and dotted lines for Brozifoot (1972) and for Neckel and Labs (1981). The region shortward of 2640Å has been enlarged by a factor of 10 for clarity.

IV. HIGH RESOLUTION SPECTRA

As with the data for absolute calibration, it has been necessary to obtain the high resolution data from several sources in order to cover the desired wavelength range. Since line strengths and shapes vary from the center of the solar disc to the limb, it is necessary to have high resolution data which refer to the whole disc. This drastically limits the number of available sources of data. As noted above, we require for our purposes a spectral resolution of order 1 km/sec (10 mÅ at 3000 Å) and a corresponding accuracy for the wavelength scale.

A. λ3800 – 7000 Å

For most of the optical range we have adopted the atlas of Beckers et al. (1976) taken at Sacramento Peak Observatory (Sac Peak hereafter). This spectrum was obtained by using a cylindrical lens of only 5 mm focal length to image the sun onto the entrance slit of a double-pass spectrometer. The spectrometer was used with two different gratings in 8th to 15th orders with 100 Å interference filters to isolate the order of interest. The data (in the magnetic tape version of the atlas) are sampled at 5 mÅ intervals. The resolving power was approximately 300,000 for the range from λ4000 – 7000 Å (13 mÅ at 4000 Å ~ 1 km/sec) and 192,000 for the range λ3800 – 4000 Å (21 mÅ at 4000 Å, ~ 1.5 km/sec). To reduce noise, the data were additionally smoothed with a Gaussian filter of width at the e^{-1} point $\pm \lambda/750,000$ (10 mÅ at 4000 Å). As noted in the introduction to that atlas, there should be no fine structure at higher resolution than this because of solar rotation.

The original atlas was normalized to a continuum intensity of 0.9, but because they carried out the scans in small sections (10 – 20 Å each) there

may be errors of several percent in defining the continuum level near strong Fraunhofer lines.

Because many of our calculations involve wavelengths deduced from molecular constants and because we are combining both optical and ultraviolet data, it was decided to use all wavelengths in vacuum. Since the Sac Peak Atlas uses wavelengths in air, it was necessary to convert the wavelength scale. For equally spaced values of λ_{vac} we calculated λ_{air} from

$$
\lambda_{vac}/\lambda_{air} = 1 + 10^{-6}\{64.328 + 29498.1/[146 - 1/\lambda_v^2] \\
+ 255.4/[41-1/\lambda_v^2]\} \tag{1}
$$

using λ in microns (c.f., Allen 1973, p. 124). The flux from the Sac Peak Atlas was interpolated to this wavelength in air.

B. $\lambda 3000 - 4050$ Å

Data for this spectral range were obtained by R. A. West at Kitt Peak National Observatory using the Fourier Transform Spectrometer (FTS) at the McMath Solar Telescope. This instrument provides full-disc spectra at high spectral resolution. The three original interferograms were taken on 21 and 22 June 1981 with the sun near transit to minimize losses due to the severe atmospheric attenuation at these wavelengths. They cover three separate but overlapping spectral regions to produce spectra covering the regions: a. (2887 - 3435 Å), b. (3233 - 3977 Å) and c. (3487 - 4057 Å). The maximum airmasses were 1.05, 1.21, and 1.30 for a, b, and c, respectively. Because of the filters used to prevent aliasing in the interferograms, the signal dropped essentially to zero near the ends of these spectral ranges and the full range

is not useful. Each interferogram consisted of ~ 7×10^5 points yielding a resolving power near 3.5×10^5 or a resolution near 10 mÅ.

The spectra, as obtained on magnetic tape from G. Ladd at Kitt Peak, were interpolated to 0.005 Å intervals (vacuum wavelengths) and the overlap regions plotted to check for consistency. The agreement in the overlap regions was excellent so the spectra were merged, after applying the absolute calibration, into a single spectrum using a linear weighted average in the overlap regions. In other words, between 3240 and 3400 Å , the weighting varied linearly from 100% spectrum a/0% spectrum b at 3240 Å to 0% spectrum a/100% spectrum b at 3400 Å and similarly between 3520 and 3960 Å for spectra b and c.

No attempt was made to explicitly correct for atmospheric attenuation. Attentuation varying slowly with wavelength is automatically removed during the application of the absolute calibration. Discrete absorption features, e.g., due to telluric O_3, may still remain. Because of our interest in OH, the spectral region from 3070 to 3085 Å was carefully compared with the spectrum of the center of the disc measured with a rocket by Kohl, Parkinson, and Kurucz (1978). No discrete telluric features could be identified in this region. However, features of significant strength may exist in other wavelength regions.

C. $\lambda 2250 - 3050$ Å

For this spectral region we have utilized the atlas of Kohl, Parkinson, and Kurucz (1978, KPK hereafter). This atlas contains spectra of the center of the disc and of a position near the limb ($\mu = 0.23$). The spectral resolution is 0.028 Å, slightly coarse for our needs but still the most appropriate data available. In addition, the wavelength scale itself is accurate only to about 0.02 Å, another significant limitation from our point

of view. The magnetic tape version of the atlas is tabulated, however, at 5 mÅ intervals of wavelength in air.

Kohl et al. (1980) have used the KPK atlas to derive total solar irradiance by assuming a shape for the limb darkening curve and assuming that the spectrum for the center of the disk is valid for the interval $1.0 > \mu >$ 0.23 and that the spectrum for the limb is valid over the interval from $0.23 > \mu \geq 0.0$. Since we are applying a separate absolute calibration, we need only the relative weights of the two spectra but in earlier work we did try to maintain the absolute intensity calibration of the KPK atlas. Using the limb-darkening coefficients of Allen (1973, p. 171) we deduced the weighting

$$
I_\lambda = 0.545 \ I_{\mu=1} + \begin{cases} 0.330 \ I_{\mu=0.23} \\ 0.080 \ I_{\mu=1} \ (\text{if } I_{\mu=0.23} \text{ is not given}) \end{cases}
$$

$$(2)$$

The second form is needed over selected wavelength intervals in which KPK do not give a spectrum for the limb. Most of these regions are at the longer wavelengths and it is for this reason that we have discarded all data from KPK for $\lambda > 3050$ Å.

The comparison of the solar spectral irradiance deduced from this atlas with many other sources has been discussed in some detail by Kohl et al. (1980) and will not be repeated here. The atlas wavelengths were converted from air to vacuum and interpolated to uniform 5 mÅ intervals in vacuum wavelength.

V. THE COMBINED ATLAS

Each of the three high resolution atlases (and each piece of the KPNO atlas) was independently placed on our absolute scale before they were combined into a single atlas. The atlas was integrated over each bandpass of the absolute calibration, Table 1, and divided into the calibration value (already in units of radiation density at r = 1 AU). Each quotient was associated with the wavelength at the center of the corresponding bandpass and the set of quotients defined the calibration curve for the high resolution spectrum. These points were then fitted with a cubic spline to define a continuous calibration function and were multiplied by the high resolution atlas to provide a final absolutely calibrated atlas. The response curves are shown in Figure 2.

To combine the three atlases, we first checked for wavelength shifts between them by calculating the cross-correlation function between each pair of absolutely calibrated, high resolution spectra for all 5 Å intervals in the overlap region between the spectra. These cross-correlation functions are shown in Figure 3 and indicate both that there are wavelength shifts of order 10 mÅ between the spectra and that there is noise in the wavelength scales of order 5 mÅ. An average of the offsets shown in Figure 3 yields $\lambda_{KPNO} - \lambda_{KPK} = -0.0206 \pm .0045$ Å (rms) and $\lambda_{KPNO} - \lambda_{SP} = -0.0119 \pm .0013$ Å (rms). Note that the variations in the cross-correlation functions are much greater for KPNO vs. KPK than for KPNO vs. Sac Peak. This is consistent with the wavelength errors quoted by KPK. A comparison with laboratory wavelengths in the overlap region of Kitt Peak and Sac Peak indicated that the Sac Peak wavelength calibration was better. Therefore, we shifted the Kitt Peak spectrum redward by 0.01 Å (exactly 2 data points). This procedure is not correct since the wavelength scale of an FTS spectrum will be in error by only a multiplicative
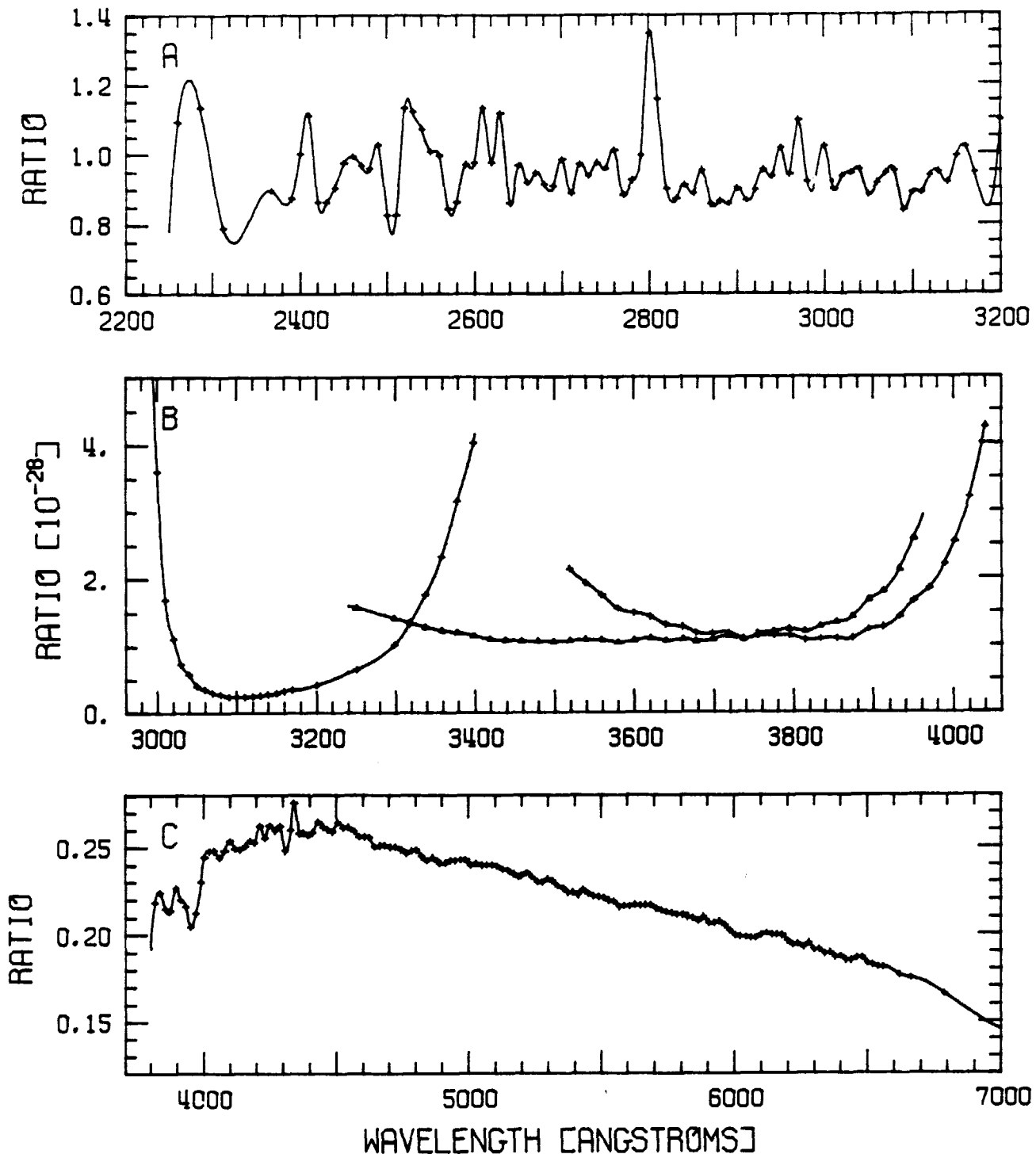
Figure 2: Response curves used for the absolute calibration of (A) the KPK
atlas, (B) the Kitt Peak atlas (three individual scans), and (C) the Sac Peak
atlas. Data points are the ratio between the absolute calibrations at the
center of a band pass and the high resolution atlas integrated over this same
band pass. A cubic spline fitted through these data points yields the
continuous calibration function. The scale for the ordinate in (B) has an
unusual exponent because the Kitt Peak scans had no previous calibration
applied to them. The largest deviations from a smooth curve are all
associated with strong, solar absorption features.
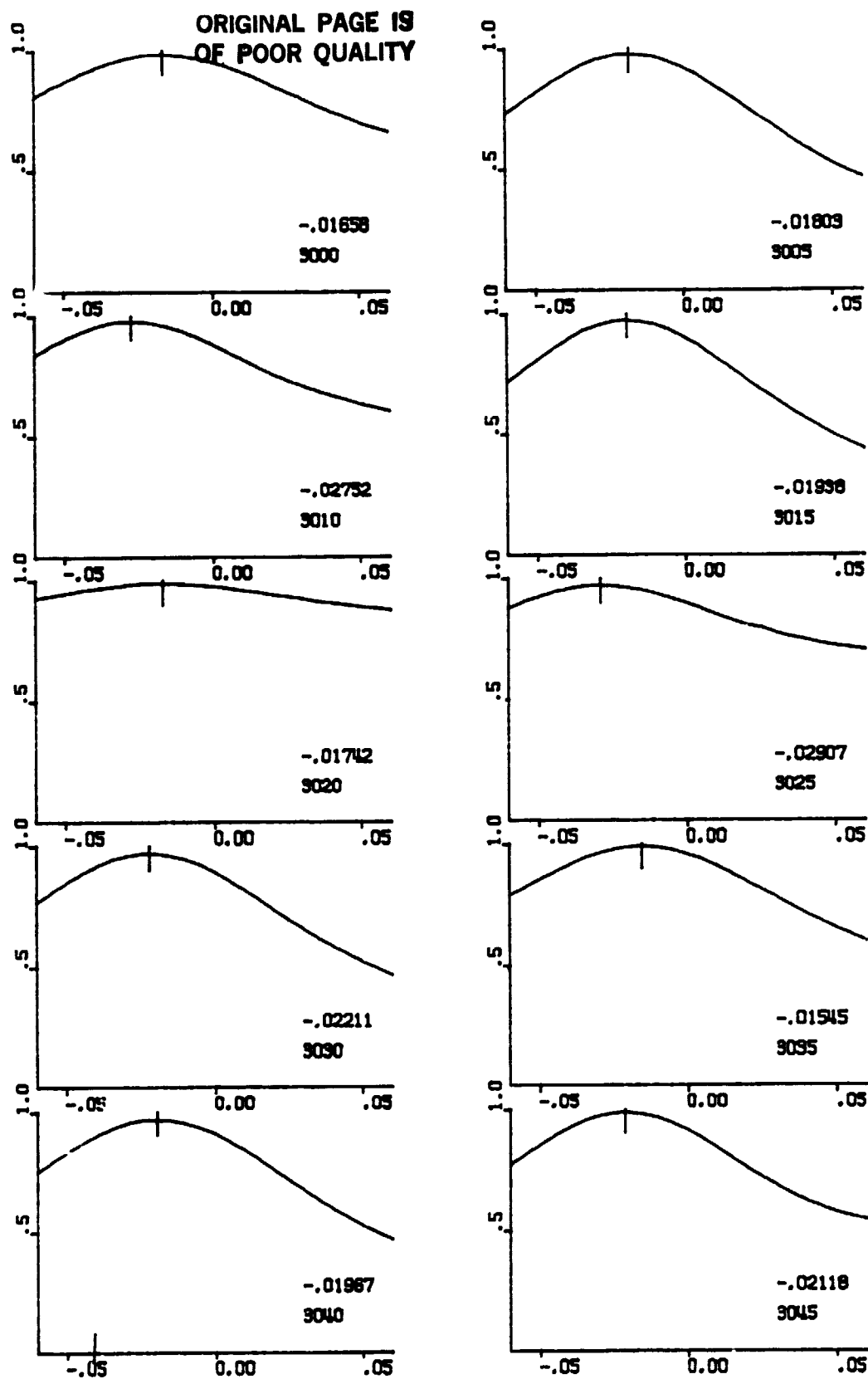
Figure 3A: Cross-correlation between Kitt Peak and KPK atlases for each 5Å interval in the overlapping region. The peaks, indicated by the vertical tic marks, show the wavelength offset between the two atlases. Each panel is labelled by the offset and by the shortest wavelength in the 5Å interval. Average offset is -0.0206Å with 0.0045Å (rms) fluctuation.

-.01148
3900

-.01124
3905

-.01252
3910

-.01206
3915

-.01117
3920

-.01140
3925

-.01038
3930

-.01197
3935

-.01133
3940

-.011'9
3945

Figure 3B: Cross-correlation between KPNO and Sac Peak atlases for each 5Å
interval in the overlapping region. The peaks, indicated by the vertical tic
marks, show the wavelength offset between the two atlases. Each panel is
labelled by the offset and by the shortest wavelength in the 5Å interval.
Average offset is -0.0119Å with 0.0013Å (rms) variation.

-.01048

3950

-.00955

3955

-.01094

3960

-.01244

3965

-.01157

3970

-.01311

3975

-.01229

3980

-.01328

3985

-.01449

3990

-.01474

3995

Figure 3B -- continued.

factor, but as the difference in the shift between 3000 and 4000 Å would be significantly smaller than our desired resolution we opted for the simpler approach of a constant shift. To bring the KPK atlas into agreement both with the KPNO atlas and with laboratory wavelengths over the range 3000 to 3050 Å, we shifted the KPK atlas blueward by 0.01 Å.
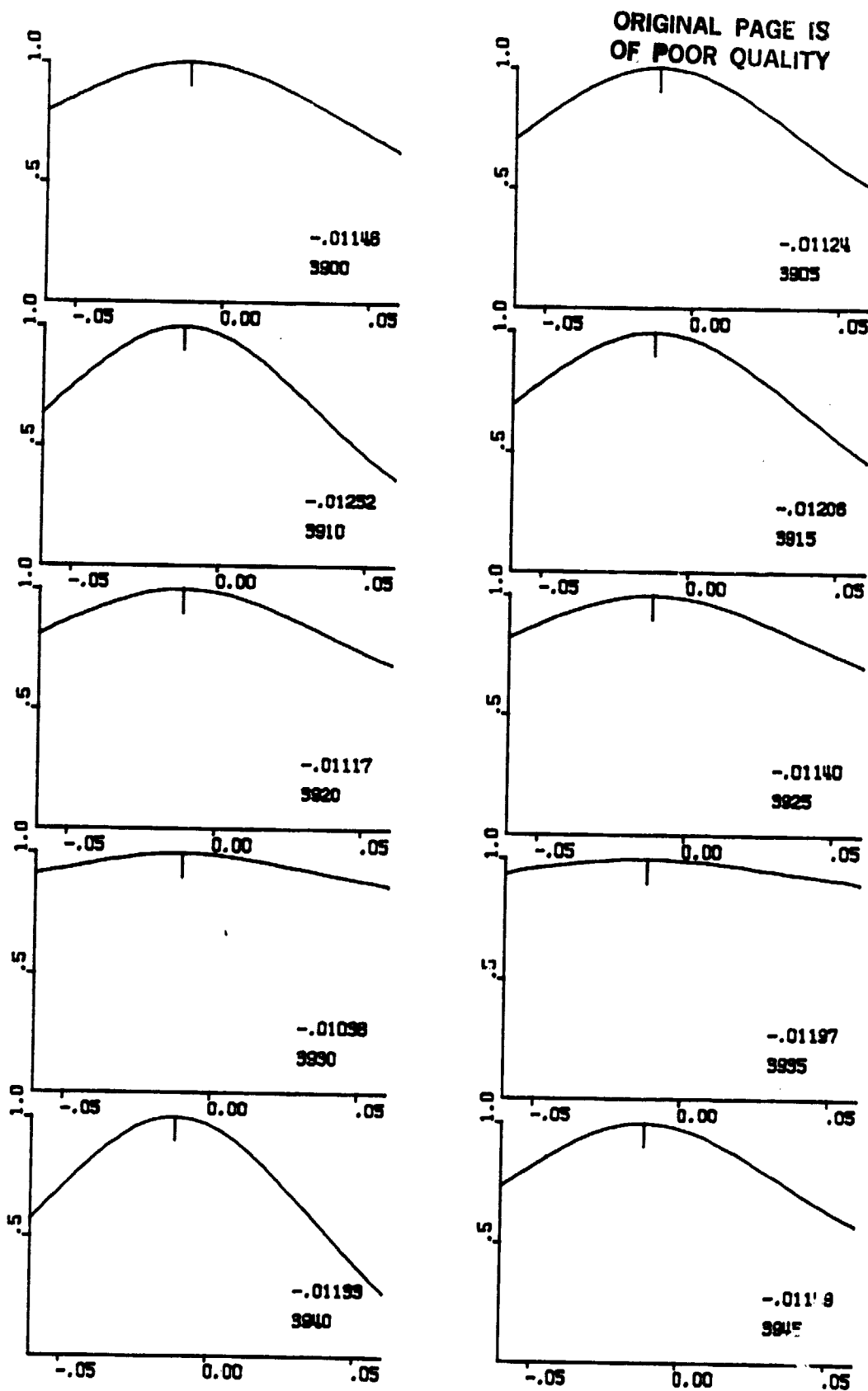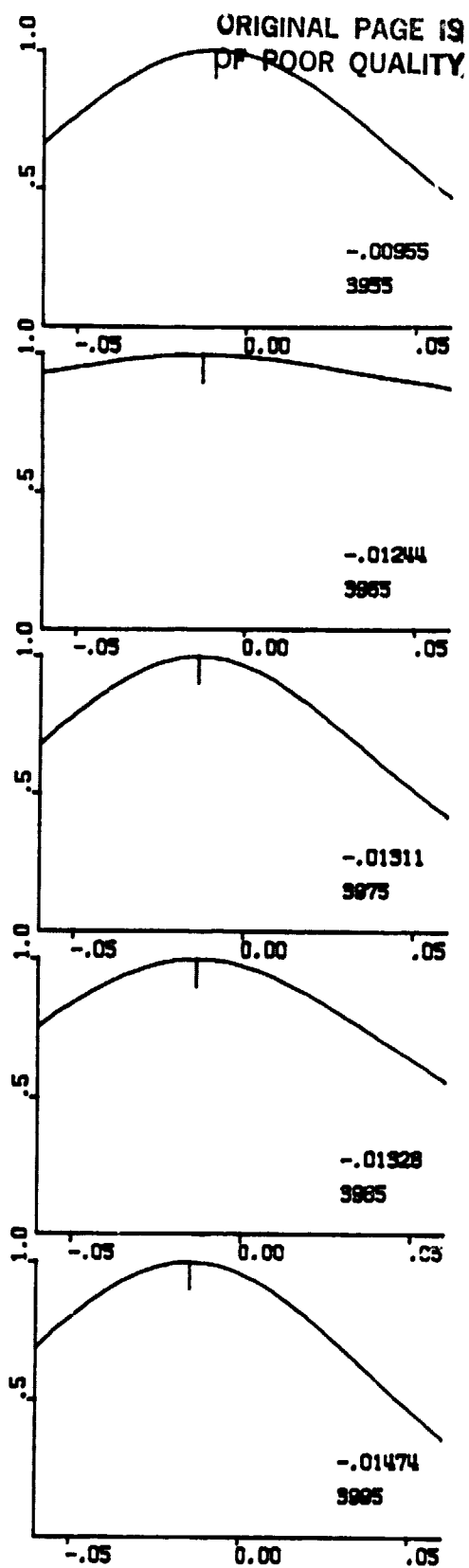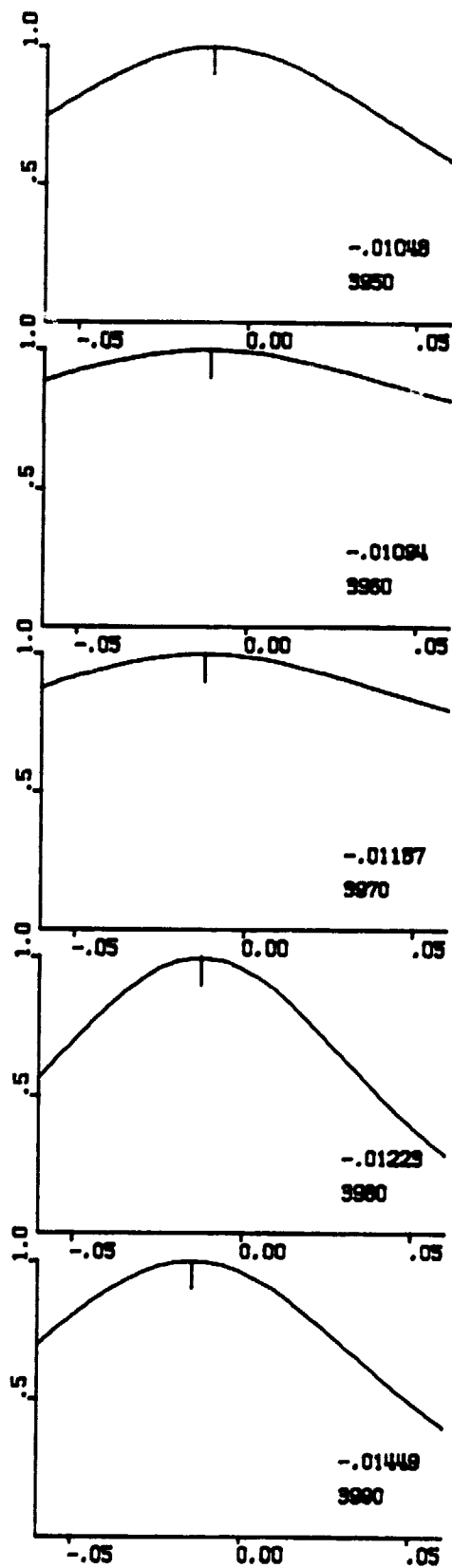
Finally, we used a linearly varying weighting function to merge the three atlases in their overlap regions. The weighting functions used varied from 100% KPK/0% KPNO at 3000 Å to 0% KPK/100% KPNO at 3050 Å and from 100% KPNO/0% Sac Peak at 3900 Å to 0% KPNO/100% Sac Peak at 4000 Å.

In Figure 4 we show portions of the overlap regions of the final spectra, showing both original sources after application of the wavelength shifts described above. Note that even over the scale of a few Angstroms there is significant jitter in wavelength when KPK and KPNO are compared; when KPNO and Sac Peak are compared, the jitter in wavelength is less than our wavelength spacing of 5 Å. This suggests that the final atlas may have wavelength uncertainties significantly greater than the spacing, perhaps up to 10 or 20 mÅ, for wavelengths less than 3050 Å but not for longer wavelengths.

We will point out only one comparison of our atlas with others. Donn, Cody, Kumar, and Wiant (private communication) have utilized a precedure similar to ours but with totally independent data to obtain a corresponding atlas. Their high resolution spectrum was obtained at Kitt Peak by Kumar and they used the absolute solar irradiance of Mount and Rottman (1981). Thus far they have calibrated only a portion of their atlas, viz the region from 3000 to 3200 Å. Wiant has carried out a point by point comparison between our two atlases for the few Angstroms in the vicinity of the strongest OH absorption. He finds excellent agreement between the two atlases with the largest differences amounting to approximately 10% of the continuum.
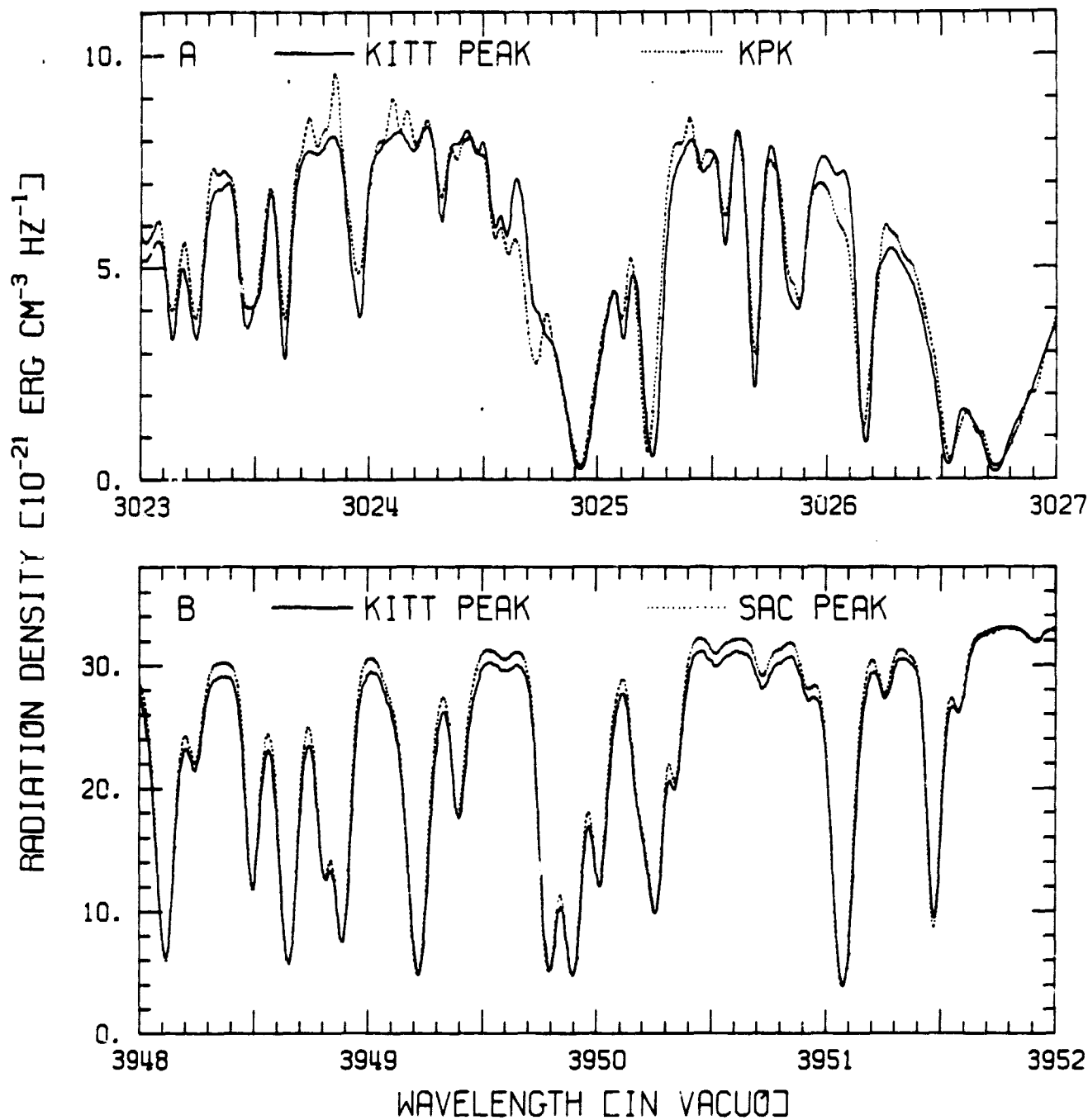
Figure 4: The middle of the overlap region of (A) Kitt Peak (solid) and KPK (dotted) atlases and of (B) Kitt Peak (solid) and Sac Peak (dotted) atlases after absolute calibration and application of the wavelength shifts described in the text.

This portion of our spectrum is shown in Figure 5 where we have superimposed the positions of the five absorption transitions which dominate the ultraviolet pumping of OH. For comparison purposes, we also show a spectrum based solely on the center-of-disc spectrum of KPK which we used in a previous study of OH fluorescence (Schleicher and A'Hearn, 1982). The differences are significant and are due to several factors including the change from center-of-disc to whole disc, the systematic shift in wavelength, the reduced jitter in wavelength of the KPNO data, and the new absolute calibration.

We conclude that our atlas can be used for calculations of fluorescent spectra with confidence. The uncertanties in the solar flux should generally not be the limiting factors in the accuracy of the resultant spectra although the wavelength errors shortward of 3050 Å may lead to errors in deduced fluxes greater than 10%.
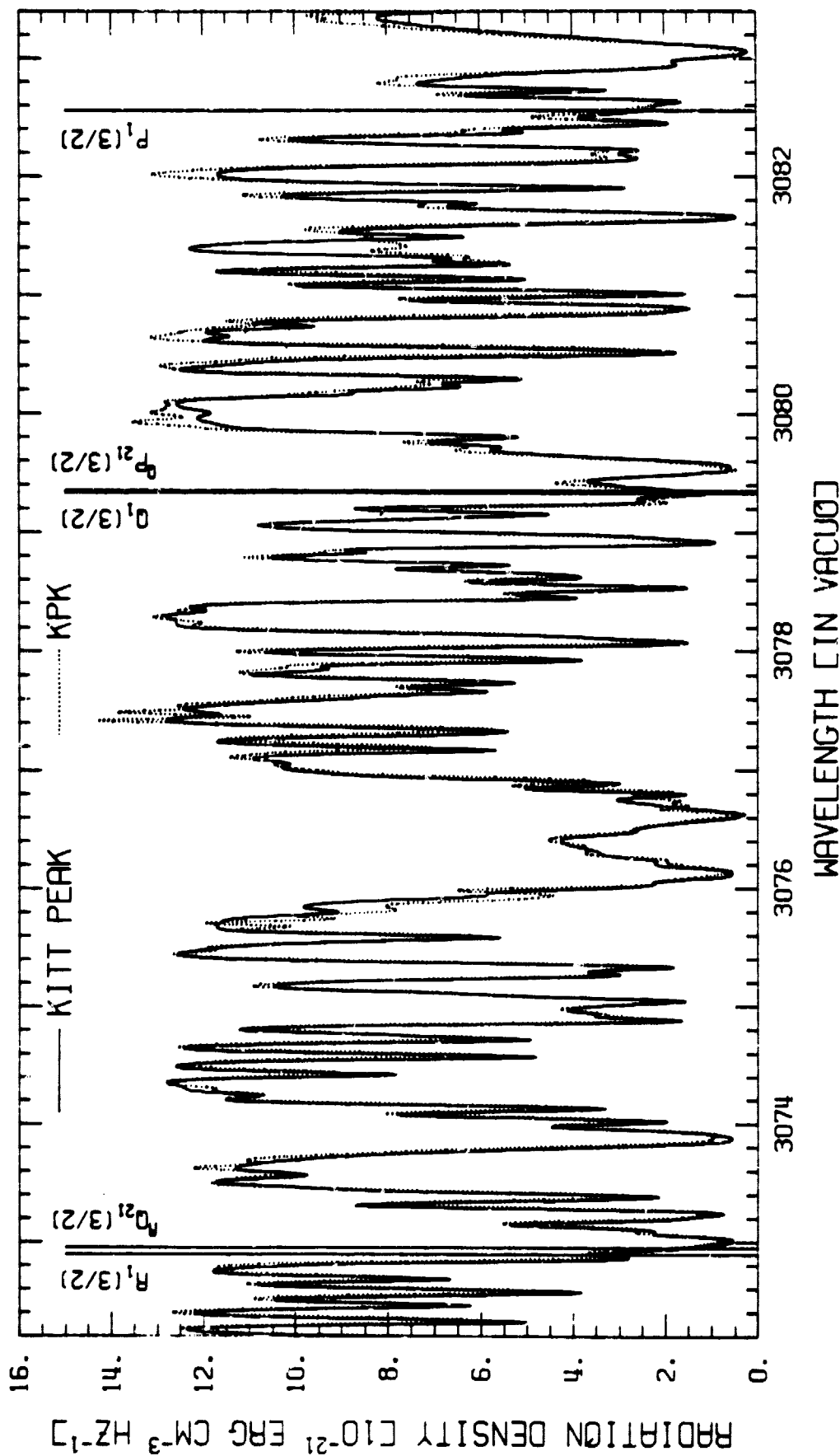
Figure 5: The major lines of the $A^2\Sigma^+ - X^2\Pi$ 0-0 band of OH arising from the ground state – which dominate the fluorescence process in cometary OH – are overlaid on our adopted solar spectrum (solid) and on the original KPK atlas, used in our previous OH fluorescence calculation (Schleicher and A'Hearn 1982). The KPK atlas shown has been shifted from air to vacuum wavelengths and converted to units of radiation density at 1 AU. Line positions are for zero Doppler shift; a change of heliocentric radial velocity of 10 km s^{-1} corresponds to approximately a 0.1Å shift.

VI. AVAILABILITY

The final magnetic tape version of the atlas is available from the authors. Our own tape is 9-track, written in UNIVAC 1180 binary format. We will also provide tapes written in ASCII upon request. The data are blocked in records of 1002 words each, with the first two words being the number of data points in the record (always 1000) and the wavelength in Angstroms of the first point. The remaining 1000 words are the radiation densities at 1 AU (erg cm^{-3} Hz^{-1}) at intervals of 0.005 Å. Thus each record covers 5 Å. A graphical version of the portion of the atlas covering $\lambda 2250 - 4000$ Å will also be available. The portion of the atlas longward of 4000 Å is not available from us in graphical form, since it differs from the previously published atlas (Beckers et al. 1976) only by a wavelength shift (air to vacuum) and the smoothly varying response curve of Figure 2. Potential users needing either the magnetic tape or the graphical display should contact the authors to make arrangements for reproduction of copies.

VII. ACKNOWLEDGEMENTS

REFERENCES

Allen. C.W., (1973). "Astrophysical Quantities," 3rd edition, (London: Athlone Press).

Beckers, Jacques M., Charles, A. Bridges, and Lou R. Gillian (1976). "A High Resolution Spectral Atlas of the Solar Irradiance from 380 to 700 Nanometers." Air Force Geophysical Laboratory Publication, AFGL-TR-76-0126.

Broadfoot, A. Lyle (1972). "The Solar Spectrum 2100 - 3200 Å." Ap. J., 173, 681-689.

Fröhlich, Claus (1981). "The Variability of the Solar Output." In Variations of the Solar Constant, ed., S. Sofia (NASA CP-2191, U.S. Govt. Print. Off.) pp. 37-44.

Hardorp, Johannes (1980). "The Sun Among the Stars. III. Energy Distribution of 16 Northern G-Type Stars and the Solar Flux Calibration." Astron. Astrophys., 91, 221-232.

Kohl, John L., William H. Parkinson, and Robert L. Kurucz (1978). "Center and Limb Solar Spectrum in High Spectral Resolution 225.2 nm to 319.6 nm." (Cambridge: Harvard-Smithsonian Center for Astrophysics)

Kohl, John L., William H. Parkinson, and Carlos A. Zapata (1980). "Solar Spectral Radiance and Irradiance at 225.2 - 319.6 Nanometers", Ap. J. Suppl. Ser., 44, 295-317.

Labs, Dietrich and Heinz Neckel (1968). "The Radiation of the Solar Photosphere from 2000 Å to 100 μ." Zs. f. Ap., 69, 1-73.

Livingston, W., H. Holwoger, and O.R. White (1981). "Observed Variability in the Fraunhofer Line Spectrum of Solar Flux, 1975 - 1980." In Variations of the Solar Constant., ed. S. Sofia (NASA CP-2191, U.S. Govt. Print. Off.) pp. 95-109.

Mount, George H. and Gary J Rottman (1981). "The Solar Spectral Irradiance 1200 - 3184 Å Near Solar Maximum: July 15, 1980." J.G.R., 86, 9193-9198.

Mount, George H., Gary J. Rottman, and J. Gethyn Timothy (1980). "The Solar Spectral Irradiance 1200 - 2550 Å at Solar Maximum." J.G.R., 85, 4271 - 4274.

Neckel, Heinz and Dietrich Labs (1981). "Improved Data of Solar Spectral Irradiance from 0.33 to 1.25 μ." Solar Phys., 74, 231-249.

Nicolet, Marcel (1981). "The Solar Spectral Irradiance and its Action in the Atmospheric Photodissociation Process." Planet. Space Sci., 29, 951-974.

Schleicher, David G. and Michael F. A'Hearn (1981). "OH Fluorescence in Comets: Fluorescence Efficiency of the Ultraviolet Bands." Ap. J., 258, 864-877.

Simon, P. (1975). "Nouvelles mesures de l'ultraviolet solaire dans la stratosphère." Bull. Acad. Roy. Belg. (Class. Sci.), 61, 399-409.

Simon, Paul C. (1981). "Solar Irradiance Between 120 and 400 nm and its Variations." Solar Physics, 74, 273-291.

Simon, Paul C., Roger Pastiels, and Dennis Nevejans (1982). "Balloon Observations of Solar Ultraviolet Irradiance at Solar Minimum." Plan. Space Sci., 30, 67-71.

Smith, Elske v.P. and David M. Gotlieb (1974). "Solar Flux and Its Variations." Space Sci. Rev., 16, 771-802.

Table 1: Adopted Absolute Calibration of the Sun at Low Resolution

λ_1 [Å]	λ_2 [Å]	ρ_ν [10^{-24}ergcm^{-3}Hz^{-1}]	Source[1]
2247.2	2272.7	277	SPN
2272.7	2298.9	317	SPN
2298.9	2325.5	261	SPN
2352.9	2381.0	302	SPN = .830B
2385.0	2395.0	304	.847B
2395.0	2405.0	273	.861B
2405.0	2415.0	274	.875B
2415.0	2425.0	445	.888B
2425.0	2435.0	476	.902B
2435.0	2445.0	460	.916B
2445.0	2455.0	383	.930B
2455.0	2465.0	362	.943B
2465.0	2475.0	417	.957B
2475.0	2485.0	394	.971B
2485.0	2495.0	367	.985B
2495.0	2505.0	504	B
2505.0	2515.0	420	B
2515.0	2525.0	344	R
2525.0	2535.0	393	B
2535.0	2545.0	475	B
2545.0	2555.0	575	B
2555.0	2565.0	718	B
2565.0	2575.0	1005	R
2575.0	2585.0	1055	B
2585.0	2595.0	1002	R
2595.0	2605.0	776	B
2605.0	2615.0	704	R
2615.0	2625.0	950	B
2625.0	2635.0	889	R
2635.0	2645.0	2036	B
2645.0	2655.0	2026	B
2655.0	2665.0	2199	B
2665.0	2675.0	2112	B
2675.0	2685.0	2156	R
2685.0	2695.0	2039	B
2695.0	2705.0	2268	B
2705.0	2715.0	2246	B

2715.0	2725.0	1605	B
2725.0	2735.0	1991	B
2735.0	2745.0	1284	B
2745.0	2755.0	1337	B
2755.0	2765.0	2013	B
2765.0	2775.0	2259	B
2775.0	2785.0	1683	R
2785.0	2795.0	1104	B
2795.0	2805.0	737	B
2805.0	2815.0	1490	B
2815.0	2825.0	2480	B
2825.0	2835.0	2902	B
2835.0	2845.0	2768	B
2845.0	2855.0	1354	B
2855.0	2865.0	2604	B
2865.0	2875.0	3374	B
2875.0	2885.0	2692	B
2885.0	2895.0	3870	B
2895.0	2905.0	5420	B
2905.0	2915.0	5580	B
2915.0	2925.0	5060	B
2925.0	2935.0	5200	B
2935.0	2945.0	4890	R
2945.0	2955.0	4980	B
2955.0	2965.0	5610	B
2965.0	2975.0	4290	B
2975.0	2985.0	5020	B
2985.0	2995.0	4790	B
2995.0	3005.0	4210	B
3005.0	3015.0	4720	$1.004B$
3015.0	3025.0	4140	$1.008B$
3025.0	3035.0	6330	$1.012B$
3035.0	3045.0	5930	$1.016B$
3045.0	3055.0	6410	$1.020B = .075B + 0.25S$
3055.0	3065.0	5360	$1.029B$
3065.0	3075.0	6080	$1.038B$
3075.0	3085.0	6360	$1.047B$
3085.0	3095.0	5560	$1.056B$
3095.0	3105.0	5130	$1.065B = .0.50B + 0.50S$
3105.0	3115.0	7940	$1.080B$
3115.0	3125.0	6730	$1.094B$
3125.0	3135.0	7150	$1.108B$
3135.0	3145.0	7510	$1.123B$
3145.0	3155.0	7500	$1.138B = 0.25B + 0.75S$
3155.0	3165.0	6170	$1.153B$

3165.0	3175.0	8840	1.168B
3175.0	3225.0	8540	S
3225.0	3275.0	11010	S
3287.9	3308.4	13470	1.060NL = 0.33NL + 0.67S
3307.4	3327.9	12440	1.055NL
3327.7	3348.2	12070	1.051NL = 0.59NL + 0.41S
3348.3	3368.8	11550	1.037NL
3368.4	3388.9	11220	1.018NL
3388.0	3408.5	12640	NL
3408.4	3428.9	12150	NL
3427.7	3448.2	11270	NL
34 ° 0	3468.5	12260	NL
3468.3	3488.8	12530	NL
3487.9	3508.4	13070	NL
3508.3	3528.8	13080	NL
3528.7	2549.2	15700	NL
3548.8	3569.3	14850	NL
3569.1	3589.6	10610	NL
3589.3	3609.8	15310	NL
3609.9	3630.4	15210	NL
3630.3	3650.8	14620	NL
3650.8	3671.3	18740	NL
3667.5	3688.0	17300	NL
3688.0	3708.5	18270	NL
3708.4	3728.9	17860	NL
3726.4	3746.9	14920	NL
3744.5	3765.0	16020	NL
3765.0	3785.5	21510	NL
3784.1	3804.6	19220	NL
3803.7	3824.2	18130	NL
3823.3	3843.8	11950	NL
3843.5	3864.0	16620	NL
3863.5	3884.0	16280	NL
3883.9	3904.4	19310	NL
3901.7	3922.2	21590	NL
3922.2	3942.7	12850	NL
3940.0	3960.5	22040	NL
3959.0	3979.5	15160	NL
3979.0	3999.5	27740	NL
3990.8	4011.3	29570	NL
4010.0	4030.0	32100	NL
4030.0	4050.0	29450	NL
4050.0	4070.0	30180	NL
4068.8	4088.8	31310	NL
4088.8	4108.8	31030	NL

4107.1	4127.1	34200	NL
4127.1	4147.1	33000	NL
4146.5	4166.5	34380	NL
4165.9	4185.9	32840	NL
4181.2	4201.2	32370	NL
4201.2	4221.2	35880	NL
4221.0	4241.0	32860	NL
4237.5	4257.5	35150	NL
4257.9	4277.9	32830	NL
4276.·	4296.4	33710	NL
4296.4	4316.4	25380	NL
4316.4	4336.4	37350	NL
4329.7	4349.7	36390	NL
4349.2	4369.2	39230	NL
4361.9	4381.9	39200	NL
4381.9	4401.9	35910	NL
4399.0	4419.0	38790	NL
4418.0	4438.0	42660	NL
4437.2	4457.2	42860	NL
4454.0	4474.0	41050	NL
4473.2	4493.2	45170	NL
4493.2	4513.2	48060	NL
4513.6	4533.6	45450	NL
4533.6	4553.6	46240	NL
4553.6	4573.6	47710	NL
4573.7	4593.7	47130	NL
4593.7	4613.7	47670	NL
4613.6	4633.6	49820	NL
4633.6	4653.6	47850	NL
4653.6	4673.6	47340	NL
4673.5	4693.5	49080	NL
4693.5	4713.5	47820	NL
4713.3	4733.3	50100	NL
4733.3	4753.3	50870	NL
4753.3	4773.3	49780	NL
4773.3	4793.3	52200	NL
4793.3	4813.3	52980	NL
4813.3	4833.3	52840	NL
4833.1	4853.1	52510	NL
4853.1	4873.1	45130	NL
4873.1	4893.1	49810	NL
4882.9	4902.9	51660	NL
4902.9	4922.9	50590	NL
4922.9	4942.9	52390	NL
4941.5	4961.5	54260	NL

4960.7	4980.7	54800	NL
4978.9	4998.9	53200	NL
4998.9	5018.9	50900	NL
5018.9	5038.9	54080	NL
5038.9	5058.9	54330	NL
5058.3	5078.3	56220	NL
5078.3	5098.3	55520	NL
5098.3	5118.3	56090	NL
5118.3	5138.3	55450	NL
5138.3	5158.3	54630	NL
5158.3	5178.3	50280	NL
5178.3	5198.3	51900	NL
5189.5	5209.5	54680	NL
5209.3	5229.3	57010	NL
5228.8	5248.8	58430	NL
5248.0	5268.0	56340	NL
5268.0	5288.0	56040	NL
5288.0	5308.0	60620	NL
5306.5	5326.5	60820	NL
5325.2	5345.2	58380	NL
5343.9	5363.9	61790	NL
5362.0	5382.0	59380	NL
5381.5	5401.5	59590	NL
5400.0	5420.0	58780	NL
5420.0	5440.0	62380	NL
5440.0	5460.0	60840	NL
5460.0	5480.0	61370	NL
5480.0	5500.0	62620	NL
5498.0	5518.0	2720	NL
5517.3	5537.3	63000	NL
5537.0	5557.0	64390	NL
5556.9	5576.9	62080	NL
5576.9	5596.9	62490	NL
5596.9	5616.9	63100	NL
5616.9	5636.9	65290	NL
5636.0	5656.0	64870	NL
5656.0	5676.0	65080	NL
5676.0	5696.0	66080	NL
5696.0	5716.0	64810	NL
5716.0	5736.0	68310	NL
5736.0	5756.0	67680	NL
5756.0	5776.0	68120	NL
5774.5	5794.5	67100	NL
5794.5	5814.5	68970	NL
5814.5	5834.5	69600	NL

5834.5	5854.5	69660	NL
5854.5	5874.5	68480	NL
5874.0	5894.0	67220	NL
5893.7	5913.7	67420	NL
5913.5	5933.5	69350	NL
5933.5	5953.5	70230	NL
5953.5	5973.5	71060	NL
5973.0	5993.0	68960	NL
5993.0	6013.0	69140	NL
6013.0	6033.0	68840	NL
6033.0	6053.0	71450	NL
6053.0	6073.0	71040	NL
6070.0	6090.0	71150	NL
6090.0	6110.0	71210	NL
6110.0	6130.0	72430	NL
6130.0	6150.0	71280	NL
6150.0	6170.0	70460	NL
6170.0	6190.0	73300	NL
6190.0	6210.0	73350	NL
6209.7	6229.7	72760	NL
6229.0	6249.0	71760	NL
6249.0	6269.0	72270	NL
6269.0	6289.0	73760	NL
6289.0	6309.0	72400	NL
6309.0	6329.0	73300	NL
6329.0	6349.0	73390	NL
6349.0	6369.0	74550	NL
6369.0	6389.0	75270	NL
6389.0	6409.0	73830	NL
6409.0	6429.0	73780	NL
6429.0	6449.0	74730	NL
6449.0	6469.0	74820	NL
6469.0	6489.0	75290	NL
6489.0	6509.0	73520	NL
6509.0	6529.0	75750	NL
6529.0	6549.0	75670	NL
6549.0	6569.0	65720	NL
6611.0	6631.0	76790	NL
6653.0	6673.0	76560	NL
6780.0	6800.0	75380	NL

NOTE:
1. Sources are: SPN = Simon, Pastiels, and Nevejans (1982)
                      B = Broadfoot (1972)
                      S = Simon (1975)
                     NL = Neckel and Labs (1981)